



Published in final edited form as:

Mutat Res. 2009 June 1; 665(1-2): 67–74. doi:10.1016/j.mrfmmm.2009.03.004.

Centrosomal amplification and aneuploidy induced by the antiretroviral drug AZT in hamster and human cells

Jennifer P. Borojerdi^{1,*}, Jessica Ming^{1,*}, Catherine Cooch¹, Yvona Ward², Cristina Semino-Mora³, Mia Yu¹, Hannan M. Braun¹, Barbara J. Taylor¹, Miriam C. Poirier¹, and Ofelia A. Olivero^{1,**}

¹Laboratory of Cancer Biology and Genetics, CCR, NCI, NIH, Bethesda, MD 20892

²Cell and Cancer Biology Branch, CCR, NCI, NIH, Bethesda, MD 20892

³Laboratory of Gastrointestinal and Liver Studies, Department of Medicine, Uniformed Services University of the Health Sciences, Bethesda, MD 20814, USA

Abstract

The centrosome directs chromosomal migration by a complex process of tubulin-chromatin binding. In this contribution centrosomal abnormalities, including centrosomal amplification, were explored in Chinese Hamster Ovary (CHO) and Normal Human Mammary Epithelial (NHMEC) cells exposed to the antiretroviral drug zidovudine (3'-azido-3'-deoxythymidine, AZT). Centrosomal amplification/fragmentation was observed in both cell types and kinetochore positive micronuclei were found in AZT-exposed CHO cells in correlation with dose. Normal human mammary epithelial cell (NMHEC), strain M99005, previously identified as a strain that incorporates high levels of AZT into DNA (High incorporator, HI), showed greater centrosomal amplification when compared with a second strain, NHMEC M98040, which did not incorporate AZT into DNA (Low incorporator, LI). Additionally, an abnormal tubulin distribution was observed in AZT-exposed HI cells bearing multiple centrosomes. Immunofluorescent staining of human cells with Aurora A, a kinase involved in the maturation of the centrosome, confirmed the induction of centrosomal amplification and revealed multipolar mitotic figures. Flow cytometric studies revealed that cells bearing abnormal numbers of centrosomes and abnormal tubulin distribution had similar S-phase percentages suggesting that cells bearing unbalanced chromosomal segregation could divide. Therefore, AZT induces genomic instability and clastogenicity as well as alterations in proteins involved in centrosomal activation, all of which may contribute to the carcinogenic properties of this compound.

Keywords

kinetochore; aurora A; aurora B; immunohistochemistry; zidovudine; flow cytometry; confocal microscopy; pericentrin

**Corresponding author National Cancer Institute, NIH, 37 Convent Dr. MSC 4255 Bldg 37 Rm 4032 Bethesda MD 20892-4255 Voice 301-435-7843 Fax 301-402 0153 Electronic mail address: E-mail: oliveroo@exchange.nih.gov.

*These authors contributed equally to the manuscript.

Publisher's Disclaimer: This is a PDF file of an unedited manuscript that has been accepted for publication. As a service to our customers we are providing this early version of the manuscript. The manuscript will undergo copyediting, typesetting, and review of the resulting proof before it is published in its final citable form. Please note that during the production process errors may be discovered which could affect the content, and all legal disclaimers that apply to the journal pertain.

Introduction

The centrosome is an organelle that regulates migration of chromosomes to the daughter cells, and is also a microtubule organizer. Based on the multiple proteins residing in the centrosome-associated protein matrix, centrosomes have been implicated in other cellular functions including cell-cycle transitions, such as G₁ to S-phase, G₂ to mitosis and metaphase to anaphase [1,2]. Cells normally have one centrosome, which duplicates synchronously with the phases of the cell cycle to generate two new centrosomes, each of which is comprised of a pair of orthogonally placed centrioles. Inhibition of centrosomal duplication generates incomplete mitotic spindles lacking cell polarity. Conversely, a multiplicity of centrosomes will generate aberrant mitotic spindles with chromosomes migrating to numerous poles, hence causing aneuploidy. Most human carcinomas have an abnormal centrosomal number that contributes to the genomic instability characteristic of transformed cells [3-6]. Additionally, it has been reported that malfunction of the centrosome induces delay in the G₁-S progression of the cell cycle [7,8].

Zidovudine (3'-azido-3'-deoxythymidine, AZT), the first nucleoside reverse transcriptase inhibitor (NRTI) used for HIV-1 therapy has been shown to induce micronuclei, chromosomal aberrations, mutations and telomeric attrition *in vitro* and *in vivo* [9,10]. Additionally AZT becomes incorporated into eukaryotic DNA [11,12] and induces cell cycle arrest with accumulation of cells in S-phase [13-17]. Since AZT has been shown to be a transplacental carcinogen of moderate potency in mice [10,11] it is important to understand the mechanisms underlying the carcinogenic potential of this drug.

Here, we report for the first time the ability of AZT to act as a centrosome disruptor. By immunohistochemistry (IHC), hamster CHO cells and human NHMEC strains, exposed to AZT for 24 hr, showed centrosomal disruption evidenced by pericentrin staining and multipolar mitotic figures, with additional aberrations in tubulin polymerization in cells bearing abnormal centrosomes. In addition, the presence of kinetochore positive micronuclei suggest the potential of the drug to act as an aneugen. The consequences of these events and their occurrence at therapeutic concentrations in human patients remain to be established.

Materials and Methods

Culture, exposure and cytotoxicity of normal human mammary epithelial cells (NHMECs)

NHMECs were cultured from organoids derived from tissues obtained at reduction mammoplasty by the Cooperative Human Tissue Network. The NHMEC strains used here have been previously characterized [18]. Cells were grown at 37°C in 5% CO₂ and serum free Mammary Epithelial Cell Medium (Cambrex, Rockland, ME) supplemented with growth factors, insulin and pituitary extracts (Cambrex). AZT (Sigma-Aldrich Co, St Louis, MO) was dissolved in phosphate buffered saline (PBS) pH 7.2 (Biosource, Rockville, MD) and the final concentration was calculated from absorbance at 266 nm with a molar extinction coefficient of 11,500. Two NHMEC strains were selected for these experiments, based on their ability to incorporate AZT into DNA [19]. Low incorporator (LI) strain M98040 cells and high incorporator (HI) strain M980005 cells were cultured for 6 passages, grown to 75% confluency and exposed in duplicate for 24 hours to 0, 10 or 200 µM AZT. For survival studies, cells were seeded in triplicate, trypsinized, and a fraction of the cell suspension was counted in a Coulter Particle Counter (Model Z1, Coulter Electronics, Luton, UK). Cell survival was expressed as percentage of viable cells in comparison to the unexposed control.

Culture, exposure and cytotoxicity of Chinese Hamster Ovary (CHO) cells

CHO cells, obtained from the American Type Culture Collection (ATCC, Manassas, VA), were cultured in HAM F12 medium (Lonza Walkersville, Inc. Walkersville, MD) and supplemented with 10 % Fetal Bovine Serum (ATCC), and antibiotics. For cytotoxicity assays, 75% confluent monolayers of CHO cells were exposed to 0, 200, 400 or 800 μM AZT for 24 hr on in duplicate experiments and processed as described above. CHO has been the cell line of choice for this study because centrosome re-duplication occurs despite blockade of DNA synthesis. With the aim of establishing if normal human cells are affected by NRTI treatment, NHMECs were used. The selection of two NHMECs strains with different abilities to incorporate AZT, due to their TK-1 status aimed to determine the role of AZT in the induction of centrosomal amplification.

Aberrant mitotic figures in CHO cells

CHO cells, seeded in 4-chamber slides (BD Biosciences, Bedford, MA) at a density of 20,000 cells/well were treated in duplicate experiments with 0, 200, 400 and 800 μM AZT for 20 hours. AZT was removed and cells were allowed to progress to mitosis for an additional 4 hours. Slides were washed with PBS and fixed with 70% alcohol for 15 min. Scoring of multipolar mitoses and lagging chromosomes was performed in 500 cells stained with Giemsa.

CHO and NHMEC centrosomal integrity determined by immunohistochemistry (IHC) staining

CHO cells and the two NHMEC strains, HI and LI were seeded in 4-chamber slides. CHO cells were exposed as described above. NHMECs were exposed to 0 and 200 μM AZT for 24 hr. For both cell types medium was removed and cells were washed 2 times with PBS and once with PBS-Tween (0.05%). Monolayers were fixed with ice cold methanol for 30 min at -20°C , followed by washes with PBS-Tween, and extraction by 0.1% Triton-X100 in 1X PBS for 4 minutes. Slides were then blocked with 2% BSA in PBS for 1 hr. Anti-pericentrin (Covance, Emeryville, CA, 1:300 dilution) and anti- β -tubulin (Sigma-Aldrich, 1:200 dilution) were used as primary antibodies for 2 hours at room temperature. Following washes in PBS-Tween, the secondary antibodies, anti-rabbit Alexa 488 (Invitrogen, Carlsbad, CA) for pericentrin, and anti-mouse rhodamine red for tubulin (Invitrogen), were applied for 30 min. DAPI (Invitrogen), was used to visualize DNA [20]. Staining by this procedure will produce blue nuclei (DAPI), red tubulin (rhodamine red) and punctate green centrosomal signals (Alexa 488) throughout the cytoplasm. A total of 1,200 cells with visible centrosomes was scored for each treatment group for both the CHO cells and the NHMEC strains.

Centrosomal integrity in CHO cells determined by transmission electron microscopy (TEM)

CHO cells seeded in 6-well plates were exposed to 0, 200, 400 and 800 μM AZT for 24 hours. After incubation, cells were scraped, collected by centrifugation, fixed for 2 hours with 2.5 % glutaraldehyde (Polysciences Inc., Warrington, PA) and post-fixed in 1% osmium tetroxide for 1h at 4°C . Cells were then dehydrated by ethyl alcohol, incubated with propylene oxide, and embedded with Spurr's low viscosity embedding mixture (Polysciences Inc.). Polymerized blocks were obtained after an overnight incubation at 70°C . Semi-thin sections of 0.5 μm stained with toluidine blue were used to select the best preserved structures which were then further trimmed to 500 \AA thin sections, stained with uranyl acetate and lead citrate and observed under a CM 100 Philips electron microscope (TEM) at 80kv (Core facility, USUHS). Electron micrographs were obtained and scanned for further ultrastructural analysis. Numbers of centrosomes and pericentriolar satellites were counted *in situ*, in the TEM screen at a 10,500 X magnification, in predetermined areas identified at low magnification as containing centrioles. In order to avoid counting repeated areas during morphometric analysis, only 1 of the 3 grids was analyzed for each experimental condition, and only 1 of 15 whole sections was

studied in each grid [21,22]. A total of 50 untreated cells, 60 cells exposed to 400 μM AZT and 55 cells exposed to 800 μM AZT were scored.

Aurora A and Aurora B staining in NHMECs

NHMECs cultured in 4-well polystyrene chamber slides were exposed to 0, 10 or 200 μM AZT for 24 hours, fixed with ice cold methanol for 30 min at -20°C , and washed with PBS-Tween. Cells were permeabilized for 5 min with 0.025% SDS and 0.1% Triton in PBS, washed with PBS-Tween and blocked for 1 hr at room temperature (Blocking solution: 10% goat serum, 1% BSA, 0.02% sodium azide in PBS) before incubation with: a rabbit polyclonal anti-Aurora A antibody (Cell Signaling Technology, Inc. Danvers, MA) at 1:250 dilution in 1% BSA in TBS solution (Tris Buffer Saline :0.05 M Tris-HCl 0.15 mM NaCl, pH 7.6.), at 4°C overnight; or a rabbit polyclonal anti-Aurora B antibody (Abcam, Cambridge, MA) at 1:200 dilution in 1% BSA in PBS/Tween solution at 4°C , overnight. An anti-rabbit Alexa 488-conjugated antibody (Invitrogen) was used as the secondary antibody at a 1:500 dilution for Aurora A or a 1:400 dilution for Aurora B, for 30 min at room temperature. DAPI was used to visualize DNA. Additionally, percentage of cells in different phases of the mitosis was scored in ~ 4000 cells from which 200 NHMEC were mitotic, exposed to 200 μM AZT stained with Aurora B (Table IV). The star indicates statistical significance ($p=0.002$) for that group compared with the corresponding unexposed controls.

CHO and NHMEC kinetochore staining by IHC

CHO cells and NHMECs cultured in 4-well polystyrene chamber slides, were fixed with ice cold methanol for 30 min at -20°C and permeabilized for 4 min with 0.1% Triton-x100 in PBS. Then cells were incubated overnight at 4°C with human anti-kinetochore CREST (calcinosis, Raynaud's phenomenon, esophageal dysfunction, sclerodactyly, telangiectasia) antibody (Antibodies Incorporated, Davis, CA) at a 1:40 dilution in blocking solution. Slides were washed as above and incubated for 90 min at room temperature with anti-human Alexa 488 (Invitrogen 1:500) secondary antiserum in blocking solution (10% goat serum, 0.01% Sodium azide, 1% Bovine serum albumin in PBS). DAPI was used to visualize nuclei and micronuclei [23]. Scoring of 1000 cells per treatment allowed identification of micronuclei with or without kinetochore (CREST) positive green signals.

Fluorescent and Confocal Microscopy

For fluorescence microscopy cells were visualized and analyzed using a Nikon Eclipse E-400 (Nikon, Inc, Melville, NY) microscope fitted with a Plan Apo 100x objective with a 1.40 numerical aperture. Stained cells were photographed on a Zeiss Axiovert 100M microscope equipped with a Zeiss Plan Apochromat 100x/1.4 oil Dichromic objective. Confocal images were generated using a Zeiss LSM 510 scanning laser microscope. The LSM 510 zoom software was used to produce a final magnification of 2000x. Images shown are 3-dimensional maximal projections generated from a series of images through the Z-plane.

Flowcytometric analysis of NHMEC cell cycle in cells with abnormal tubulin polymerization

NHMECs, exposed to 10 and 200 μM AZT for 24 hr in T75 flasks, were trypsinized and pelleted by centrifugation at 860g for 5 min. Fixation was accomplished by adding ice-cold methanol to pre-chilled cells with gentle vortexing, incubation on ice for 30 min and then centrifugation and resuspension in 0.5% BSA for 10 min at room temperature. Anti- β -tubulin antibody (1:25 dilution, Cell Signaling Technology, Inc.) was added and suspensions incubated for 60 min at room temperature. After washing and spinning, cells were incubated with Alexa Fluor 488 goat anti-rabbit IgG (H+L) (Invitrogen) at a 1:1000 dilution for 30 min at room temperature. Finally, cells were washed, incubated with RNase (Qiagen, Valencia, CA) and stained with propidium iodide 10 $\mu\text{g}/\text{ml}$ (Sigma-Aldrich) at 4°C , overnight. Cells were analyzed on a FACSCalibur

flow cytometer (BD Biosciences, San Jose, CA) using the doublet discrimination module. Data were acquired using CellQuest Pro (BD Biosciences) software. The cell cycle was modeled using ModFit software (Verity Software, Topsham, ME) and tubulin was measured using FlowJo software (TreeStar, Ashland, OR).

Statistical analysis

Results were expressed as mean \pm SE of three separate experiments unless otherwise indicated. The Student's t-test was used for statistical analysis for the scoring of centrosomal amplification by EM, and ANOVA was used to obtain statistical significance in percentage of mitotic phases in CHO cells (Table IV).

Results

Cytotoxicity and aberrant mitotic figures in CHO cells

For CHO cells, survival was 81.0, 71.5 and 67.5% at 24 hr of exposure for 200, 400 and 800 μ M AZT respectively. Analysis of abnormal mitotic figures was carried out in CHO cells grown in 0, 200, 400, and 800 μ M AZT for 20 hours, and then grown in AZT free media for 4 hours to permit entry into mitosis. An increase in the presence of aberrant cells, including multipolar metaphases/anaphases and cells bearing lagging chromosomes was observed in correlation with increasing doses of AZT. Table I shows the scoring of 500 Giemsa-stained cells. There were no abnormal cells in the unexposed cultures, and average percentages of 0.8%, 1.8% and 5.3 % of cells with aberrant mitotic figures were found in cultures exposed in duplicate experiments to 200 μ M, 400 μ M and 800 μ M AZT, respectively.

Centrosomal abnormalities in CHO cells determined by IHC

When compared to untreated CHO cells (Figure 1 A), CHO cells exposed to 200 μ M AZT for 24 hours showed an increase in the number of pericentrin positive structures (Figure 1 B, C). Moreover, multiple signals of smaller size were observed in some cells (Figure 1 C) and defined as centrosomal fragmentation. Centrosomal abnormalities were observed in cells exposed to all doses of AZT, and were frequently accompanied by an aberrant aggregation of tubulin (red) (Figure 1 C, thin arrow). Additionally a third type of aberrant centrosomal structure involving the observation of multiple centrosomes associated together was defined as aggregation (Figure 1 C arrow head). Scoring for cells containing > 2 centrosomes is presented in Table I. Untreated cells had a 0.2% of cells bearing the abnormality, while values for abnormal cells reached 0.4%, 1.2% and 1.9% in cells exposed to 200, 400 and 800 μ M AZT, respectively.

Amplification of CHO cell centrosomes was confirmed by visualization of EM images. Figure 2 shows photomicrographs that are representative of multiple images captured and analyzed. Panel A shows cells exposed to 400 μ M AZT for 24 hours, where black arrows point to centrioles embedded in a proteinaceous pericentriolar matrix. The photos are from an area of cytoplasm close to the nucleus and contain 3 centrioles. Centrioles show cross-sectional microtubule disposition (A, white arrows), or cylindrical longitudinal and oblique orientation. Numerous small round electro-dense structures are also observed (B, white arrow head and insert). These are considered to be pericentriolar satellites, non-membranous organelles located close to the centrosome, which in some cases have organized distribution in semicircle. Panels B shows cells exposed to 800 μ M AZT for 24 hr. The centrioles (5) are indicated by black arrows and pericentriolar satellites are indicated by white arrowheads.

Scoring of 75 photos/treatment showed an increased of centrosome number in relation to the AZT concentration. These are defined as supernumerary centrosomes in (Table I) and varied from $1.1\% \pm 0.8$ in unexposed cells to $2.8\% \pm 0.8$ and $4.4\% \pm 0.5$ for 400 μ M and 800 μ M AZT respectively ($p < 0.001$). The percentage of cells showing pericentriolar satellites (Table

I), the specific electro-dense round oval structures associated with the centrosomes, also increased with AZT dose to: $4.8\% \pm 0.5$ and $7.0\% \pm 0.5$ for 400 μM and 800 μM AZT respectively ($p < 0.02$), compared with $0.4\% \pm 0.2$ in unexposed cells ($p < 0.001$).

Centrosomal abnormalities induced in NHMECs

Two NHMEC strains LI and HI were chosen for these experiments, based on their different abilities to incorporate AZT into DNA when exposed to 200 μM AZT for 24 hours. At the doses used, 10 and 200 μM , cytotoxicity was very low, with a viability of $\sim 85\%$ for both cell strains when exposed to the highest dose for 24 hrs (Table II).

NHMECs were stained with pericentrin, as described above for CHO cells, to identify centrosomal amplification and the results are shown in Table II and Figure 1 D-G. Pericentrin positive signals were scored for the total number of cells with visible centrosomes observed in both NHMEC HI and LI strains. HI Cells bearing >2 centrosomes were 6.3%, 14.8% and 21.3% of cells exposed to 0, 10 and 200 μM AZT, respectively (Table II). Figure 1 D shows unexposed HI cells, and Figure 1 E shows HI cells exposed to 200 μM AZT. LI cells bearing >2 centrosomes were 5.3%, 8.0% and 12.2 % of cells exposed to 0, 10 and 200 μM AZT respectively (Table II). Figure 1 F shows unexposed LI cells and Figure 1 G shows LI cells exposed to 200 μM AZT.

β -tubulin distribution in NHMECs with centrosomal amplification

In addition to centrosomal amplification, some NHMEC cells exposed to 200 μM AZT exhibited a decreased signal for β -tubulin (Figure 1 E). These cells were labeled pericentrin (+)/ β -tubulin(-). Cells with normal distribution of tubulin and multiple pericentrin signals, were labeled pericentrin (+)/ β -tubulin (+). It would be important to emphasize here that the nomenclature (+) or (-) refers to the lack of visible red signal in the cytoplasm and not to the lack of tubulin in the cell. An apparent lack of β -tubulin staining was observed in a large proportion of AZT-exposed LI and HI NHMECs showing centrosomal amplification. Figure 1 E (circles) shows two cells with multiple pericentrin positive bodies that lack the red signal for β -tubulin. In these cells the tubulin and pericentrin signals co-localize, as determined by the yellow signals at the centrosome. Scoring of pericentrin (+)/ β -tubulin(-) cells was performed using both NHMEC strains (Table II), and β -tubulin(-) cells appeared stained green due to lack of red signal for β -tubulin (Figure 1 H). In the HI cells there was an increase in β -tubulin(-) cells from 3.5% in the unexposed cells to 23.2 % in the AZT-exposed cells. In contrast, in the LI cells the percentage of β -tubulin (-) cells did not differ between AZT-exposed and unexposed cells (Table II).

In order to understand the nature of the aberrant tubulin staining, fixed AZT-exposed cells that had not been extracted with Triton were processed for immunohistochemistry using the anti- β -tubulin antibody. Typically Triton extraction will leave intact a system of microfilamentous bundles and the detergent-resistant cytoskeleton [24]. Two possible outcomes were expected from this experiment: 1.) un-polymerized β -tubulin could be retained in the cytoplasm of un-extracted cells and appear as a diffuse red staining, or 2.) the absence of all β -tubulin (either polymerized or un-polymerized) would result in unstained cells. In Figure 1 I, a group of un-extracted AZT-exposed HI cells shows a diffuse positive staining for β -tubulin (red color), indicating that the defect previously observed was based on inability of the protein to polymerize and not due to its absence. Hence the un-permeabilized cells retained un-polymerized tubulin and were stained with a faint red color (Figure 1 I).

Cell cycle profile in pericentrin (+)/ β -tubulin (-) cells

Flow cytometry was used to separate pericentrin (+)/ β tubulin (-) and pericentrin (+)/ β -tubulin (+) cells found in AZT-exposed and unexposed LI and HI NHMECs. The results presented

here (for HI cells only, Figure 3) revealed that the cell cycle in pericentrin (+)/ β -tubulin (-) cells is identical to that exhibited by pericentrin (+)/ β -tubulin (+) cells from the same culture. This observation is true for the unexposed cells (Figure 3a), cells exposed to 10 μ M AZT (Figure 3b) and cells exposed to 200 μ M AZT (Figure 3c). Both β -tubulin (+) and β -tubulin (-) populations, represented on the top and bottom of a, b and c panels of Figure 3 exhibited similar patterns of distribution. Figure 3 (right side) also shows values for percentages of cells in S-phase, and it is evident that both β -tubulin (+) and β -tubulin (-) cultures exposed to 200 μ M AZT had an increase in the percentage of cells in S-phase compared to unexposed controls, as previously reported [9]. Both β -tubulin (+) and β -tubulin (-) cells in S-phase were 24% with 10 μ M AZT and 42% with 200 μ M AZT. The control values were 21% and 23% for β -tubulin (-) and β -tubulin (+) respectively.

Aneuploidy assessed by kinetochore (CREST) positive micronuclei in CHO cells and NHMECs

Micronuclei induced by AZT in CHO cells and NHMECs were scored in 1,000 cells of both cell types. From those, a subset of micronuclei was found to contain kinetochore (CREST) positive signals. Figure 1J shows a CHO cell exposed to 800 μ M AZT with a kinetochore-bearing micronucleus. NHMECs, HI cells exposed to 200 μ M AZT are illustrated in Figure 1K. A kinetochore-bearing micronuclei is observed as blue (DAPI) circles containing multiple green (CREST antibody) signals, additionally Figure 1K shows a different type of aberration consisting of a large body still attached to the nucleus containing 3–4 CREST positive signals. Values for the frequency of CREST positive micronuclei are shown in Table III. An increase in the number of micronuclei from 20 to 50/1000 cells was observed in CHO cells with increasing doses of AZT, however the increase in total of CREST positive containing micronuclei was only significantly different from the controls at the highest dose of 800 μ M. In contrast NHMEC scoring demonstrated significant increases in CREST positive micronuclei in AZT-exposed LI and HI cells at both doses (Table III)

Aurora A, Aurora B and multipolar spindles in NHMECs

In addition to the evaluation of centrosomal amplification, the distribution of the centrosomal kinases Aurora A and B was examined by immunohistochemistry. NHMECs exposed to 0, 10 and 200 μ M AZT for 24 hr were stained with anti Aurora A and B antibodies. Multipolar spindles and multiple centrosomal bodies were observed in AZT-exposed NHMEC HI cells and were identified by Aurora A-positive signals in NHMECs exposed to 200 μ M AZT (Figure 1 L) and 10 μ M AZT compared to unexposed controls. Unexposed cells exhibited an average of 6.5% abnormal cells (with > 2 Aurora positive signals or multiple spindles) while 14.6% of cells exposed to 10 μ M AZT and 21.7% of 200 μ M cells were abnormal. A Western blot analysis of NHMEC lysates (Figure 4) revealed an increase in protein expression of Aurora A in HI cells with both 10 μ M and 200 μ M AZT, while in LI cells, there is a modest increase in expression induced by the high dose only. Similarly, Western blot analysis performed with Aurora B revealed a clear increase of the expression of the kinase in HI treated cells with both AZT doses (Figure 4, right panel) while LI cells did not show a change in the expression level with any dose (Figure 4, left panel).

Aurora B-stained NHMECs revealed such abundant distribution of the protein that quantitation and comparison among treatments was impossible. Nonetheless mitotic figures were scored and identified by their characteristic pattern (Table IV). Percentage of cells in prophase, metaphase, anaphase and telophase was based on observation of 2,000 cells and shown for both cell strains. A statistically significant difference in the percentage of NHMEC HI cells in prophase (25 %) was revealed in cells exposed to 200 μ M AZT compared to 15% in unexposed cells ($p=0.002$). NHMECs in LI cells did not show any significant changes in the distribution

of mitotic figures. Similarly the rest of the phases analyzed for HI cells did not show statistical significant differences (Table IV)

Discussion

The highly-effective nucleoside reverse transcriptase inhibitor AZT is a DNA replication chain terminator that induces genomic instability, cell cycle arrest, micronuclei, sister chromatid exchanges, and shortened telomeres [10]. Here we report a novel centrosomal amplification and fragmentation that occurs both in hamster and human cells and results in chromosome missegregation and aneuploidy. The ability of AZT to induce these types of aberrations is reported here for the first time in studies that employed both hamster (CHO) and human NHMECs.

In CHO cells, in addition to centrosomal fragmentation and amplification the presence of numerous pericentriolar satellites was observed. Pericentriolar satellites are described as electro-dense bodies associated with the centrosome [25] and further characterized as rich in the centrosomal protein pericentriolar material-1 (PCM-1), having a potential role in centrosomal replication. [26]. Inhibition of PCM 1 with specific antibodies revealed that the protein plays an important role in cell cycle regulation, fulfilling an essential function for cells to complete interphase [27].

Incorporation of AZT into NHMEC-DNA and characterization of the incorporators has been documented previously [19]. The deficient incorporation on LI is due to the inactivation of thymidine kinase-1 (TK-1), the enzyme needed for the initial phosphorylation of AZT. However, mitochondrial TK-2 mediated phosphorylation could have occurred facilitating AZT-DNA incorporation under the level of detection of the radioimmunoassay used in the experiments. NHMECs treated with 200 μ M AZT for 24 hr exhibited an increase in the number of centrosomes, identified by positive pericentrin signals. Furthermore, the centrosomes exhibited other anomalies such as aggregation and fragmentation that co-localized with abundant tubulin, a phenomenon that has been interpreted to indicate an altered nucleation capacity [28].

Abnormal chromosomal distribution was observed in CHO and NHMEC cells revealed by the presence of CREST positive micronucleus, (Figure 1-J-K) evidenced by increased positive signal for kinetochores within micronuclei of cells exposed to AZT. This suggests malfunctioning of the mitotic spindle and as a consequence multiple poles, generated by the migration of numerous centrosomes in an aberrant pattern instead of the typical bipolar mitotic spindle. Multipolar spindles were visualized in NHMECs with immunofluorescence staining using Aurora A, a kinase involved in the maturation of the spindle (Figure 1L). The fact that the cells divide as evidenced by cells in mitosis (Figure 1,L), indicates that in many cases centrosomal amplification does not impair cell division. However the fact that the mitosis is delayed by the presence of a significant number of prophase cells indicates an abnormality in the mitotic process.

Analysis of NHMECs showed disruption of centrosomes, accompanied by abnormal chromosome distribution and aneuploidy as demonstrated by CREST positive micronuclei; and altered ability of tubulin to polymerize. Two different strains of NHMEC were selected for these experiments, HI cells with the ability to incorporate AZT into DNA and LI cells, lacking that capacity. In both cases, cells exhibited centrosomal amplification after 24 hr of AZT exposure; however, the LI cells had less prominent centrosomal amplification suggesting that AZT-DNA incorporation could play a role in this abnormality. Additionally, a cytoskeleton disorder manifested by abnormal distribution and polymerization of tubulin was observed in 23% of the HI (Figure 1-H) cells compared to a 3.8% in LI cells exposed to 200 μ M AZT. This

last phenomenon suggested a correlation between the capacity of AZT to interact with the ability of tubulin to polymerize and the ability of the drug to incorporate into DNA. Cells exhibiting a lack of signal for β -tubulin staining [defined as pericentrin (+)/ β -tubulin (-)] were analyzed by flow cytometry and revealed a similar distribution of cells in S-phase to those with normal tubulin signal [pericentrin (+)/ β -tubulin (+)], suggesting that cells bearing centrosomal amplification and abnormal β -tubulin staining are able to cycle in a similar fashion to those with a normal β -tubulin staining.

Western blots, carried out with Aurora A and B indicated that in NHMEC, Aurora A and Aurora B protein expression was up-regulated in HI cells treated with both 10 μ M and 200 μ M AZT. No change in protein expression was observed for Aurora B in LI cells and a minor change in Aurora A was observed in cells exposed to 200 μ M AZT in LI cells (Figure 4). Dysfunctional centrosomes and insufficient tension at the kinetochore-spindle connection with subsequent mitotic arrest mediated by the Aurora B-Survivin complex have been reported [29]. Furthermore arrest in pro-metaphase has been observed as a consequence of a depletion of Survivin from the Survivin-Aurora B complex by siRNA [30]. Similarly, in our experiments a statistically significant increase in prophase figures was observed (Table IV). Staining NHMECs with Aurora B allowed the identification of cells in different phases of mitosis, and showed a statistically significant increase of cells in prophase in AZT treated HI cells (Table IV). This indicates that although the cells completed mitosis they do it abnormally, most likely due to the arrest induced by an active mitotic check point.

Aneuploidy is an expected consequence of the defects described above. CREST kinetochore positive micronuclei were observed in CHO cells and NHMECs, however a peculiar distinction should be mentioned between observations in the two cell types. Although the micronuclei observed in CHO correspond to the classical described micronuclei (separated from the main nucleus, small in size not to exceed 25 % of the nucleus), the ones found in NHMEC look somewhat different. Some of them are larger and also show a connection with the main nucleus. They resemble a protrusion of the nucleus rather than a separate body as if the protrusion would culminate in strangulation. Most of them bear CREST positive signals, in many instances, many signals have been visualized (Figure 1- K).

In summary, AZT induced centrosomal amplification is documented in hamster and human cells for the first time. Mechanistically studies performed with higher drug concentration revealed supernumerary centrosomes as well as pericentriolar satellites. Cells bearing the aberration were able to cycle in a similar fashion that unaffected cells, evidenced by the presence of multipolar mitotic figures. Both, amplification and abnormal mitotic figures were observed in the presence of therapeutically relevant doses of AZT. The presence of kinetochore bearing micronuclei suggests that unbalanced chromosomal segregation or aneuploidy takes place. It could be speculated then, that aneuploidy could be one of the mechanisms underlying the carcinogenicity of AZT. Experiments aimed to determine if this is a phenomenon exclusively linked to AZT or shared by different nucleoside analogs are in progress.

Acknowledgments

The authors would like to thank Dr. Dan Sackett from the Laboratory of Integrative and Medical Biophysics, NICHD, NIH, for guidance and critical reading of the manuscript. The work was supported, in part, by the Intramural Research Program of the NIH, National Cancer Institute, Center for Cancer Research.

Abbreviations

AZT, Azidothymidine, 3'-azido-3'-deoxythymidine
BSA, Bovine Serum Albumin
CHO, Chinese Hamster Ovary

CREST, calcinosis, Raynaud phenomenon, esophageal dysmotility, sclerodactyly, and telangiectasia
 DAPI, 4',6-diamidino-2-phenylindole dihydrochloride
 LI, Low incorporator
 HI, High incorporator
 IHC, Immunohistochemistry
 NHMEC, Normal Human Mammary Epithelial Cell
 NRTI, Nucleoside Reverse Transcriptase Inhibitor
 PBS, Phosphate buffer saline
 TBS, Tris buffer saline
 TEM, transmission electron microscopy

Reference List

1. Doxsey S, Zimmerman W, Mikule K. Centrosome control of the cell cycle. *Trends Cell Biol* 2005;15:303–311. [PubMed: 15953548]
2. D'Assoro AB, Lingle WL, Salisbury JL. Centrosome amplification and the development of cancer. *Oncogene* 2002;21:6146–6153. [PubMed: 12214243]
3. Carroll PE, Okuda M, Horn HF, Biddinger P, Stambrook PJ, Gleich LL, Li YQ, Tarapore P, Fukasawa K. Centrosome hyperamplification in human cancer: chromosome instability induced by p53 mutation and/or Mdm2 overexpression. *Oncogene* 1999;18:1935–1944. [PubMed: 10208415]
4. Lingle WL, Lutz WH, Ingle JN, Maihle NJ, Salisbury JL. Centrosome hypertrophy in human breast tumors: implications for genomic stability and cell polarity. *Proc. Natl. Acad. Sci. U. S. A* 1998;95:2950–2955. [PubMed: 9501196]
5. Pihan GA, Purohit A, Wallace J, Knecht H, Woda B, Quesenberry P, Doxsey SJ. Centrosome defects and genetic instability in malignant tumors. *Cancer Res* 1998;58:3974–3985. [PubMed: 9731511]
6. Satoh MS, Lindahl T. Enzymatic repair of oxidative DNA damage. *Cancer Res* 1994;54:1899s–1901s. [PubMed: 8137308]
7. Mikule K, Delaval B, Kaldis P, Jurczyk A, Hergert P, Doxsey S. Loss of centrosome integrity induces p38-p53-p21-dependent G1-S arrest. *Nat. Cell Biol* 2007;9:160–170. [PubMed: 17330329]
8. Hinchcliffe EH, Miller FJ, Cham M, Khodjakov A, Sluder G. Requirement of a centrosomal activity for cell cycle progression through G1 into S phase. *Science* 2001;291:1547–1550. [PubMed: 11222860]
9. Olivero OA. Mechanisms of genotoxicity of nucleoside reverse transcriptase inhibitors. *Environ. Mol. Mutagen* 2007;48:215–223. [PubMed: 16395695]
10. IARC. Monographs on the Evaluation of Carcinogenic Risks to Humans. Some antiviral and antineoplastic drugs, and other pharmaceutical agents. Vol. 76. World Health Organization. International Agency for Research on Cancer; Lyon, France: 2000. p. 73-127.
11. Olivero OA, Anderson LM, Diwan BA, Haines DC, Harbaugh SW, Moskal TJ, Jones AB, Rice JM, Riggs CW, Logsdon D, Yuspa SH, Poirier MC. Transplacental effects of 3'-azido-2',3'-dideoxythymidine (AZT): tumorigenicity in mice and genotoxicity in mice and monkeys. *J. Natl. Cancer Inst* 1997;89:1602–1608. [PubMed: 9362158]
12. Diwan BA, Riggs CW, Logsdon D, Haines DC, Olivero OA, Rice JM, Yuspa SH, Poirier MC, Anderson LM. Multiorgan transplacental and neonatal carcinogenicity of 3'-azido-3'-deoxythymidine in mice. *Toxicol. Appl. Pharmacol* 1999;15:82–99. [PubMed: 10558926]
13. Olivero OA, Tejera AM, Fernandez JJ, Taylor BJ, Das S, Divi RL, Poirier MC. Zidovudine induces S-phase arrest and cell cycle gene expression changes in human cells. *Mutagenesis* 2005;20:139–146. [PubMed: 15784690]
14. Escobar PA, Olivero OA, Wade NA, Abrams EJ, Nesel CJ, Ness RB, Day RD, Day BW, Meng Q, O'Neill JP, Walker DM, Poirier MC, Walker VE, Bigbee WL. Genotoxicity assessed by the comet and GPA assays following in vitro exposure of human lymphoblastoid cells (H9) or perinatal exposure of mother-child pairs to AZT or AZT-3TC. *Environ. Mol. Mutagen* 2007;48:330–343. [PubMed: 17358027]

15. Olivero OA, Ming JM, Das S, Vazquez IL, Richardson DL, Weston A, Poirier MC. Human inter-individual variability in metabolism and genotoxic response to zidovudine. *Toxicol. Appl. Pharmacol.* 2007
16. Viora M, Di Genova G, Rivabene R, Malorni W, Fattorossi A. Interference with cell cycle progression and induction of apoptosis by dideoxynucleoside analogs. *Int. J. Immunopharmacol* 1997;19:311–321. [PubMed: 9467750]
17. Chandrasekaran B, Kute TE, Duch DS. Synchronization of cells in the S phase of the cell cycle by 3'-azido- 3'-deoxythymidine: implications for cell cytotoxicity. *Cancer Chemother. Pharmacol* 1995;35:489–495. [PubMed: 7882457]
18. Keshava C, Whipkey D, Weston A. Transcriptional signatures of environmentally relevant exposures in normal human mammary epithelial cells: benzo[a]pyrene. *Cancer Lett* 2005;221:201–211. [PubMed: 15808406]
19. Olivero OA, Ming JM, Das S, Vazquez IL, Richardson DL, Weston A, Poirier MC. Human inter-individual variability in metabolism and genotoxic response to zidovudine. *Toxicol. Appl. Pharmacol* 2008;228:158–164. [PubMed: 18206198]
20. Peloponese JM Jr, Haller K, Miyazato A, Jeang KT. Abnormal centrosome amplification in cells through the targeting of Ran-binding protein-1 by the human T cell leukemia virus type-1 Tax oncoprotein. *Proc. Natl. Acad. Sci. U. S. A* 2005;102:18974–18979. [PubMed: 16365316]
21. Semino-Mora C, Liu H, McAvoy T, Nieroda C, Studeman K, Sardi A, Dubois A. Pseudomyxoma peritonei: is disease progression related to microbial agents? A study of bacteria, MUC2 AND MUC5AC expression in disseminated peritoneal adenomucinosis and peritoneal mucinous carcinomatosis. *Ann. Surg. Oncol* 2008;15:1414–1423. [PubMed: 18299935]
22. Semino-Mora MC, Leon-Monzon ME, Dalakas MC. Effect of L-carnitine on the zidovudine-induced destruction of human myotubes. Part I: L-carnitine prevents the myotoxicity of AZT in vitro. *Lab Invest* 1994;71:102–112. [PubMed: 7518879]
23. Emdad L, Sarkar D, Su ZZ, Boukerche H, Bar-Eli M, Fisher PB. Progression elevated gene-3 (PEG-3) induces pleiotropic effects on tumor progression: modulation of genomic stability and invasion. *J. Cell Physiol* 2005;202:135–146. [PubMed: 15389539]
24. Osborn M, Weber K. The detergent-resistant cytoskeleton of tissue culture cells includes the nucleus and the microfilament bundles 4. *Exp. Cell Res* 1977;106:339–349. [PubMed: 558885]
25. Balczon R, Bao L, Zimmer WE, Brown K, Zinkowski RP, Brinkley BR. Dissociation of centrosome replication events from cycles of DNA synthesis and mitotic division in hydroxyurea-arrested Chinese hamster ovary cells. *J. Cell Biol* 1995;130:105–115. [PubMed: 7790366]
26. Kubo A, Sasaki H, Yuba-Kubo A, Tsukita S, Shiina N. Centriolar satellites: molecular characterization, ATP-dependent movement toward centrioles and possible involvement in ciliogenesis. *J. Cell Biol* 1999;147:969–980. [PubMed: 10579718]
27. Balczon R, Simerly C, Takahashi D, Schatten G. Arrest of cell cycle progression during first interphase in murine zygotes microinjected with anti-PCM-1 antibodies. *Cell Motil. Cytoskeleton* 2002;52:183–192. [PubMed: 12112146]
28. Lingle WL, Lutz WH, Ingle JN, Maihle NJ, Salisbury JL. Centrosome hypertrophy in human breast tumors: implications for genomic stability and cell polarity. *Proc. Natl. Acad. Sci. U. S. A* 1998;95:2950–2955. [PubMed: 9501196]
29. Lens SM, Medema RH. The survivin/Aurora B complex: its role in coordinating tension and attachment. *Cell Cycle* 2003;2:507–510. [PubMed: 14504461]
30. Castedo M, Perfettini JL, Roumier T, Andreau K, Medema R, Kroemer G. Cell death by mitotic catastrophe: a molecular definition. *Oncogene* 2004;23:2825–2837. [PubMed: 15077146]

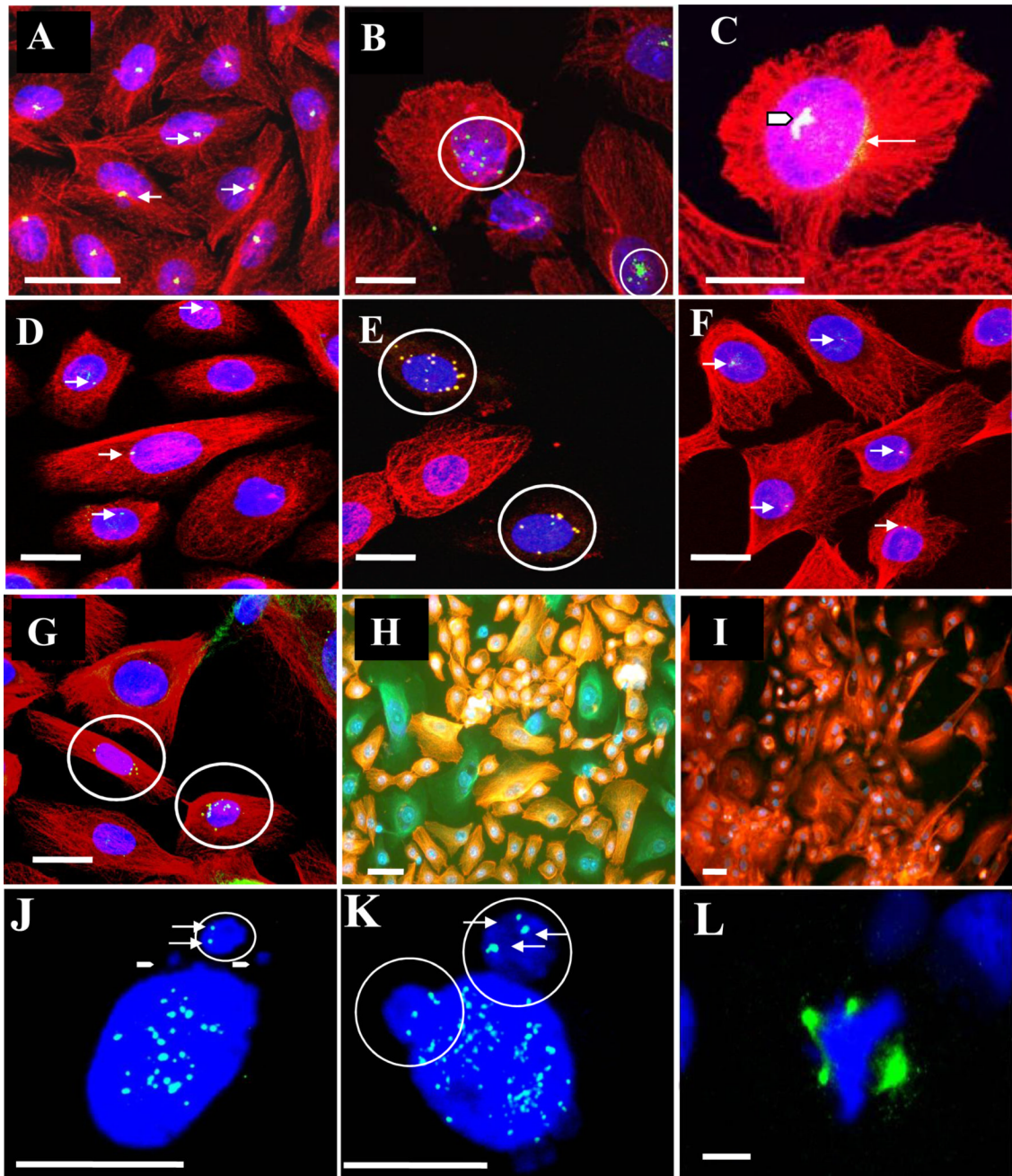
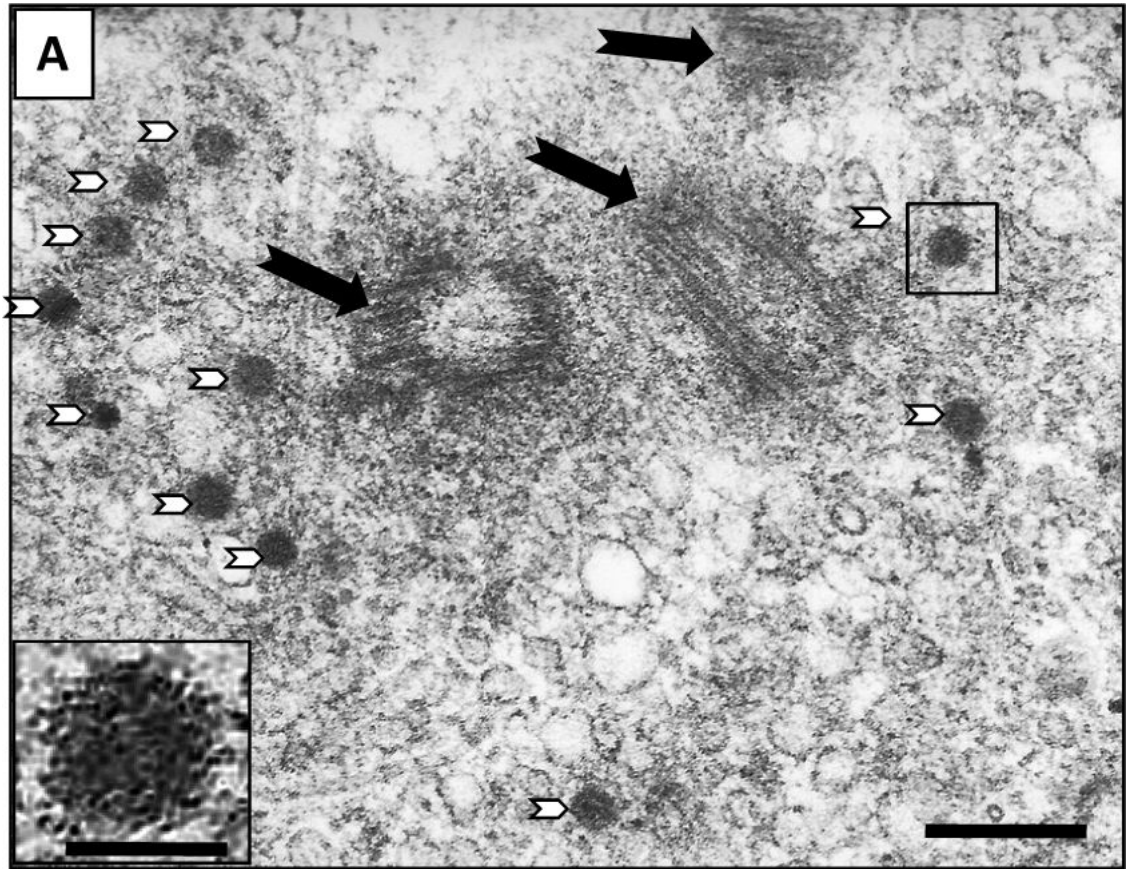


Figure 1. AZT-exposed CHO cells and, NHMEC strains visualized by confocal microscopy (A-C): CHO cells incubated with anti-pericentrin antibodies (green), anti-β-tubulin antibodies (red), and DAPI to stain DNA (blue). Co-localization of pericentrin and β-tubulin appears yellow. **(A)** Untreated cells. Arrows indicate the presence of centrosomes **(B):** CHO cells exposed to 400 μM AZT for 24 hr. Circles indicate: centrosomal amplification (top); centrosomal fragmentation multiple pericentrin-positive signals (bottom). **(C):** CHO cells exposed to 800 μM AZT for 24 hr. Arrow head indicates multiple coalescent pericentrin signals; thin white arrow indicates pericentrin aggregation. **(D-E):** NHMEC HI cells. **(D):** Untreated cells, arrows indicate centrosomes. **(E):** Cells exposed to 200 μM AZT for 24 hr, circles indicate 2 cells with amplified signal for pericentrin suggesting the presence of multiple centrosomes with co-localizing signal for tubulin. **(F-G):** NHMEC LI cells. **(F):** Unexposed

cells, arrows indicate centrosomes. **(G)**: Cells exposed to 200 μM AZT for 24 hr, circles indicate 2 cells with amplified signal for pericentrin suggesting the presence of multiple centrosomes and normal β -tubulin staining. **(H)**: NHMEC HI cells, stained with anti- β -tubulin antibodies and rhodamine (red); some cells appear green due to the lack of rhodamine staining. **(I)**: NHMEC HI cells, stained as in H but without triton extraction (soluble β -tubulin is retained in cells that have not undergone extraction). The tubulin staining red indicates that green cells in H contained un-polymerized β -tubulin. Bars = 10 μm . **(J-L)**: Kinetochore staining with CREST antibody. **(J)**: CHO cell, exposed to 800 μM AZT for 24 hr. Solid arrowheads indicate the presence of 2 small CREST-negative micronuclei, and a white circle indicates a large micronucleus with two CREST-positive kinetochores (white arrows) inside a large micronucleus. **(K)**: NHMEC HI cells showing 2 large circled bodies on top containing kinetochore positive signals (arrows). **(L)**: Triradial spindle revealed by the abnormal multipolar distribution of Aurora A, in a cell treated with 200 μM AZT for 24 hr; DAPI (blue) staining shows abnormal multipolar chromosomal distribution. Bars: J-K = 5 μm , L = 1.5 μm ,



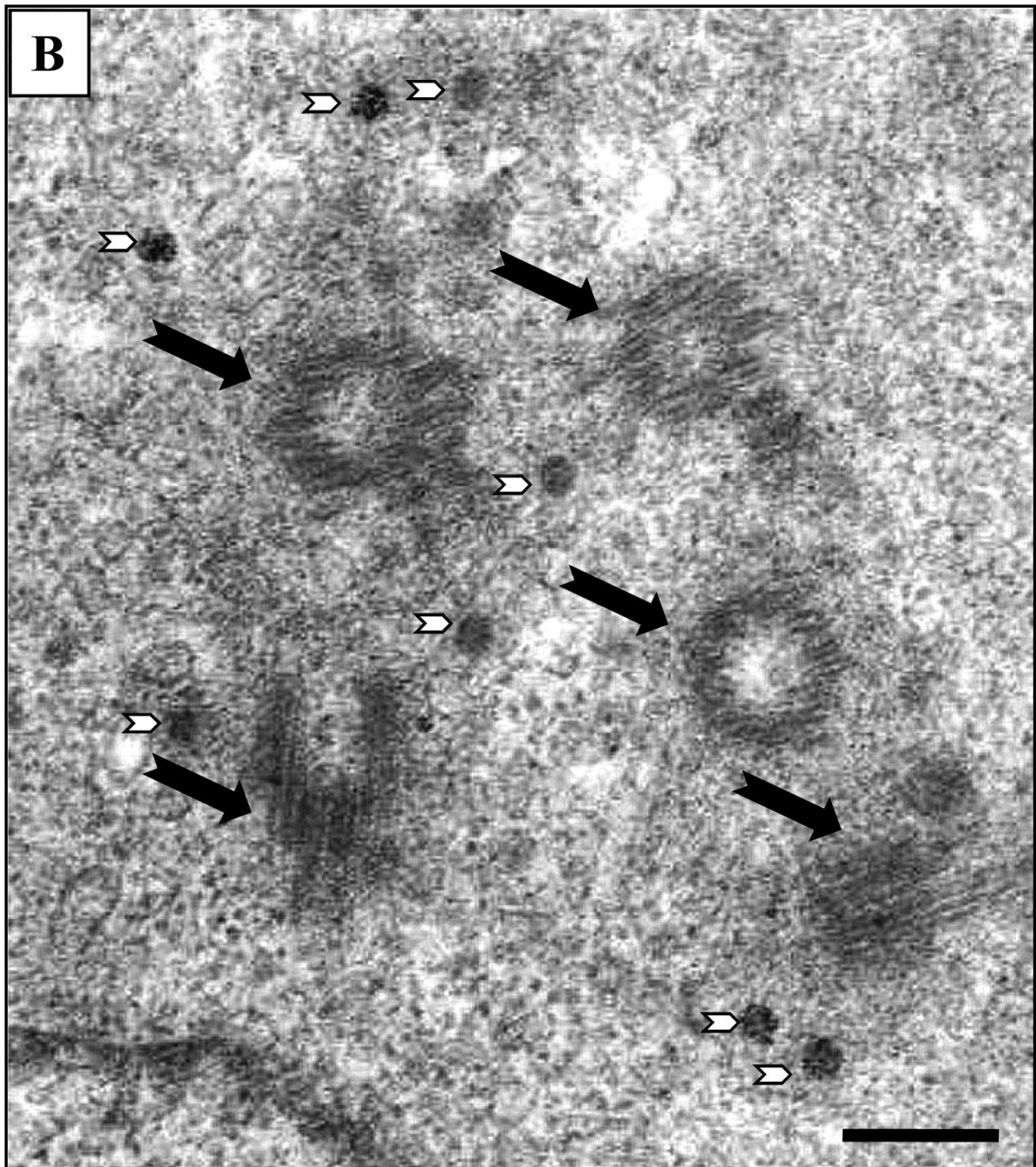


Figure 2. Electronmicroscopic images of CHO cells

(A) CHO cells exposed to 400 μM AZT for 24 hr Black arrows indicate three centrioles in cross section or cylindrical and/or oblique orientation. Numerous small round electro-dense structures are also observed (white arrowheads). Insert: detail of small round electro-dense structure indicate by a box. (B) CHO cells exposed to 800 μM AZT centrioles indicated by black arrows and pericentriolar electro-dense bodies with irregular distribution are indicated by white arrowheads. Picture bars = 200 nm, insert bar = 70 nm.

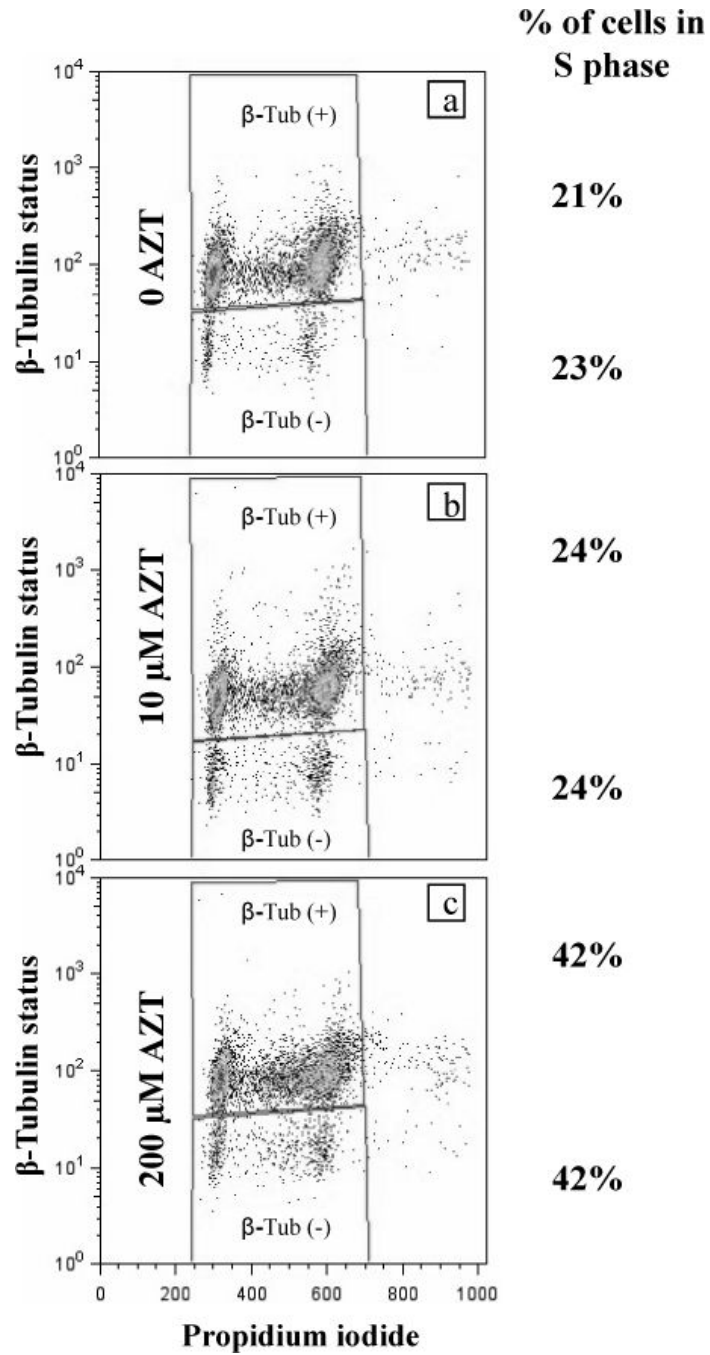


Figure 3. Flow cytometry of β -tubulin (+) and β -tubulin (-) NHMEC HI cells (a) unexposed, (b) exposed to 10 μ M AZT (c) exposed to 200 μ M AZT. Percentage of cells in S phase for both populations (top and bottom of each panel) is shown on the right. Both β -tubulin (+) and β -tubulin (-) populations show an increase in the percentage of cells in S-phase compared to unexposed controls. Cells deprived of β -tubulin staining, (bottom of each panel) and cells with positive β -tubulin staining, (top of each panel) exhibit similar patterns of distribution, hence, similar cell cycle.

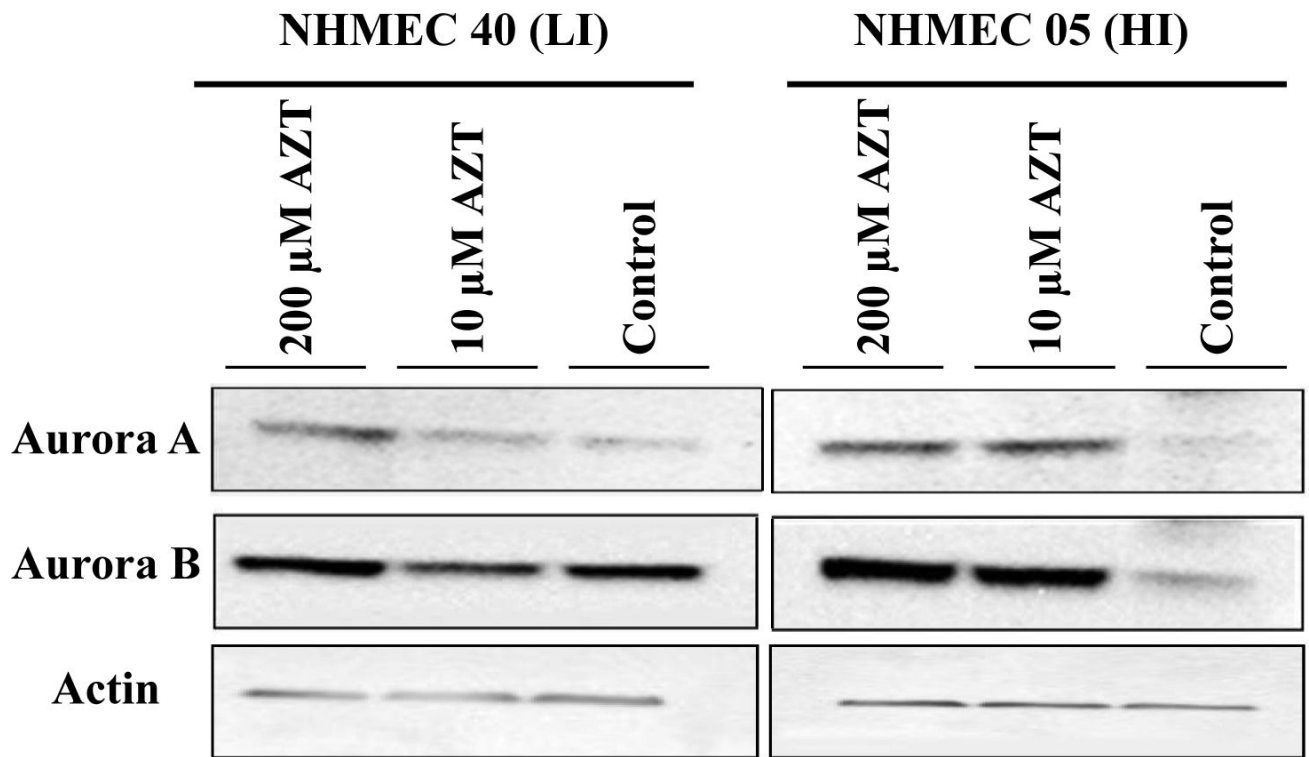


Figure 4. Western blots for Aurora A and Aurora B proteins in NHMECs

Western blot of NHMECs LI cells (left) and HI cells (right), exposed to 0, 10 and 200 μM AZT for 24 hr. Antibodies used to determine protein expression: top panel Aurora A, middle panel Aurora B and bottom panel actin.

Table I

Centrosome amplification and pericentriolar satellites in CHO cells exposed for 24 hr to AZT.

Treatment AZT μM	% cells w/ aberrant mitotic figures ^{ab}	% cells bearing > 2 centrosomes ^c	% cells w/ supernumerary centrosomes (EM)	%cells w/ pericentriolar satellites (EM) ^d
0 (control)	0	0.2	1.1 \pm 0.8	0.4 \pm 0.2
200	0.8	0.4	NA ^e	NA
400	1.8	1.2	2.8 \pm 0.8	4.8 \pm 0.5
800	5.3	1.9	4.4 \pm 0.5	6.9 \pm 0.5

^a n = 500 mitotic figures, including multipolar mitoses and cells bearing lagging chromosomes

^b mean of 2 experiments

^c n = 200 cells with visible centrosomes

^d n = 50, 60 and 55 cells with visible centrosomes for 0, 200 μM AZT and 400 μM AZT, respectively

^e NA= Not assayed

Cytotoxicity, centrosomal amplification and abnormal distribution of tubulin in NHMEC strains M99005 (HI cells) and 98040 (LI cells).

TABLE II

AZT μ M	% viable cells		% cells bearing > 2 centrosomes ^{a-b}		% cells with abnormal tubulin distribution (tubulin -) ^c	
	LI	HI	LI	HI	LI	HI
0	100	100	5.3 \pm 1.0	6.3 \pm 1.0	3.8	3.5
10 ^a	84.9 \pm 1.0	83.7 \pm 5.8	8.0 \pm 1.3	14.8 \pm 1.5	8.3	21.6
200 ^b	83.7 \pm 2.0	74.3 \pm 10.0	12.2 \pm 1.6	21.3 \pm 2.3	3.8	23.2

^aMean of 4 experiments, (n= 200 cells w/visible centrosomes)

^bMean of 3 experiments, (n= 200 cells w/visible centrosomes)

^cMean of 2 experiments, (n= 1,000 cells)

Table III
Frequency of micronuclei in CREST (+) and CREST (-) CHO cells and NHMECs^a

	CHO		NHMEC-LI		NHMEC-HI	
	CREST(+)	CREST (-)	CREST(+)	CREST (-)	CREST(+)	CREST (-)
Control	20.0	2.0	4.0	0	12.0	2.0
AZT 10 μ M	NA ^b	NA	13.0	8.0	16.0	6.0
AZT 200 μ M	25	6.0	17.0	7.5	30.5	13.0
AZT 400 μ M	18.5	5.5	NA	NA	NA	NA
AZT 800 μ M	63	17	NA	NA	NA	NA

^a A total of 6 slides and 2,000 cells, in two independent experiments were scored. Values are expressed as number of cells containing either CREST (+) or CREST (-) micronuclei/1000 cells.

^b NA = Not assayed

Table IV
Distribution of mitotic phases in NHMEC HI and LI cells exposed to 0, or 200 μ M AZT for 24 hr

	Prophase	Metaphase	Anaphase	Telophase	Total Mitosis ^(a)
HI control	15.3 \pm 1.9	4.0 \pm 1.0	3.5 \pm 0.9	18.3 \pm 2.1	41.0 \pm 3.1
HI AZT	24.9 \pm 2.5*	3.7 \pm 1.0	2.7 \pm 0.8	18.7 \pm 2.1	50.0 \pm 3.4**
LI control	22.6 \pm 2.3	5.2 \pm 1.1	2.5 \pm 0.8	16.9 \pm 2.0	47.2 \pm 3.3
LI AZT	21.6 \pm 2.3	4.2 \pm 1.0	2.7 \pm 0.8	15.4 \pm 1.9	44.0 \pm 3.2

* $p=0.002$

** $p=0.016$

^(a)Total cell scored ~4000/strain/treatment, total mitotic figures scored = 200/strain/treatment